Mammalian target of rapamycin and Rictor control neutrophil chemotaxis by regulating Rac/Cdc42 activity and the actin cytoskeleton

Yuan He[a,*], Dong Li[a,*], Sara L. Cook[a,*], Mee-Sup Yoon[a], Ashish Kapoor[b], Christopher V. Rao[b,c], Paul J. A. Kenis[b,c], Jie Chen[a,c], and Fei Wang[a,c]

[a]Department of Cell and Developmental Biology, [b]Department of Chemical and Biomolecular Engineering, and [c]Institute for Genomic Biology, University of Illinois at Urbana–Champaign, Urbana, IL 61801

ABSTRACT **Chemotaxis allows neutrophils to seek out sites of infection and inflammation. The asymmetric accumulation of filamentous actin (F-actin) at the leading edge provides the driving force for protrusion and is essential for the development and maintenance of neutrophil polarity. The mechanism that governs actin cytoskeleton dynamics and assembly in neutrophils has been extensively explored and is still not fully understood. By using neutrophil-like HL-60 cells, we describe a pivotal role for Rictor, a component of mammalian target of rapamycin complex 2 (mTORC2), in regulating assembly of the actin cytoskeleton during neutrophil chemotaxis. Depletion of mTOR and Rictor, but not Raptor, impairs actin polymerization, leading-edge establishment, and directional migration in neutrophils stimulated with chemoattractants. Of interest, depletion of mSin1, an integral component of mTORC2, causes no detectable defects in neutrophil polarity and chemotaxis. In addition, experiments with chemical inhibition and kinase-dead mutants indicate that mTOR kinase activity and AKT phosphorylation are dispensable for chemotaxis. Instead, our results suggest that the small Rho GTPases Rac and Cdc42 serve as downstream effectors of Rictor to regulate actin assembly and organization in neutrophils. Together our findings reveal an mTORC2- and mTOR kinase–independent function and mechanism of Rictor in the regulation of neutrophil chemotaxis.**

Monitoring Editor
Rong Li
Stowers Institute

Received: Jul 22, 2013
Revised: Aug 20, 2013
Accepted: Aug 23, 2013

INTRODUCTION

Chemotaxis—the ability of cells to migrate up a gradient of chemoattractant—is essential for many biological responses, including the movement of neutrophils to the sites of infection and inflammation and aggregation of *Dictyostelium discoideum* during morphogenesis. As nature's master migratory cells, neutrophils and *D. discoideum* respond to chemoattractants by adopting a highly polarized morphology, with filamentous actin (F-actin) in a protrusive leading edge. To interpret the chemoattractant gradient, a neutrophil requires a mechanism to compare signaling levels across the cell surface and restrict leading-edge activity to the most highly stimulated region. This mechanism has been referred to as the "compass" mechanism because of its ability to spatially direct actin polymerization to the leading edge (pseudopod) of protruding neutrophils (Rickert *et al.*, 2000; Bourne and Weiner, 2002; Weiner, 2002; Wang, 2009). Studies over the past decade have begun to shed light on the intracellular signals that control assembly of the actin cytoskeleton and establishment of the protruding leading edge. A special role is assigned to the phosphatidylinositol 3-kinase (PI3K) lipid product phosphatidylinositol-3,4,5-trisphosphate (PI(3,4,5)P3) in regulating chemotaxis of neutrophils and *D. discoideum*. Asymmetric localization of PI(3,4,5)P3 at the leading edge was first documented in *D. discoideum* and later in neutrophils during chemotaxis (Parent *et al.*, 1998; Meili *et al.*, 1999; Servant *et al.*, 2000; Wang *et al.*, 2002). Experiments with pi3k1/2-null *D. discoideum* and neutrophils with pharmacological inhibition suggested that PI(3,4,5)P3 is required for morphological polarity and chemotaxis (Knall *et al.*, 1997; Funamoto *et al.*, 2001; Wang *et al.*, 2002).

Although PI(3,4,5)P3 has been suggested as part of the compass mechanism in neutrophils and *D. discoideum* during chemotaxis, it

This article was published online ahead of print in MBoC in Press (http://www.molbiolcell.org/cgi/doi/10.1091/mbc.E13-07-0405) on September 4, 2013.

*These authors contributed equally to this work.

Address correspondence to: Fei Wang (feiwang@life.uiuc.edu).

Abbreviations used: dHL-60, differentiated HL-60 cells; F-actin, filamentous actin; fMLP, formyl-Met-Leu-Phe; mTORC2, mammalian target of rapamycin complex 2.

is also clear that cells still can move toward chemoattractants regardless of whether this second messenger is depleted or in excess (Hirsch *et al.*, 2000; Li *et al.*, 2000; Sasaki *et al.*, 2000; Andrew and Insall, 2007; Ferguson *et al.*, 2007; Franca-Koh *et al.*, 2007; Hoeller and Kay, 2007; Nishio *et al.*, 2007). Moreover, a study suggested that PI3K accelerates, but is not required for, neutrophil chemotaxis (Heit *et al.*, 2008). Thus cells may use parallel or completely independent pathways to direct chemotaxis. Indeed, in *D. discoideum*, deletion of a patatin-like phospholipase A2 (PLA2) homologue and two PI3Ks causes a strong defect in chemotaxis and a reduction in receptor-mediated actin polymerization, suggesting that PLA2 acts in parallel with PI3K pathways to mediate chemotaxis (Chen *et al.*, 2007). As such, neutrophils may exploit similar PI3K-independent pathway(s) to control leading-edge establishment and directional migration. The key mediators of these pathway(s) in neutrophils, however, are not known.

TOR complex 2 (TORC2) has emerged as a key regulator of the actin cytoskeleton. In budding yeast, TORC2 is resistant to rapamycin treatment and regulates bud formation (Loewith *et al.*, 2002). The homologue of yeast Torc2, mTORC2, was identified in mammals. Depletion of Rictor—a key component of mTORC2—in HeLa cells and fibroblasts disrupts stress fiber formation and reduces Rac activity (Jacinto *et al.*, 2004; Sarbassov *et al.*, 2004; Agarwal *et al.*, 2013). In *D. discoideum*, disruption of TORC2 does not affect cell survival but impairs cAMP-induced actin polymerization and chemotaxis. At a molecular level, TORC2 acts downstream of Ras and regulates phosphorylation of AKT/protein kinase B (PKB) in a PI(3,4,5)P-independent manner (Lee *et al.*, 2005; Cai *et al.*, 2010). Liu *et al.* (2010) used PLB-985 promyeloid leukemia cells as a neutrophil model and showed that Rictor is required for chemotaxis. Surprisingly, Rictor depletion only impairs actin polymerization at the late stage of chemoattractant stimulation, and instead exerts much stronger impact on the RhoA-ROCK-myosin pathway (Liu *et al.*, 2010). In the present study, we use the commonly used neutrophil-like HL-60 cells and demonstrate that mTOR and Rictor are necessary for chemoattractant-induced Rac/Cdc42 activity and actin assembly during chemotaxis. Intriguingly, depletion of mSin1, an integral component of mTORC2 (Frias *et al.*, 2006; Jacinto *et al.*, 2006; Yang *et al.*, 2006), causes no detectable defects in neutrophil polarity and chemotaxis. In addition, mTOR kinase activity and AKT phosphorylation are dispensable for neutrophil chemotaxis. Together our results suggest that Rictor regulates neutrophil polarity and chemotaxis through mTORC2- and mTOR kinase–independent mechanism(s).

RESULTS

Rictor accumulates at the leading edge of chemotactic neutrophils

Accumulating evidence has pointed to mTORC2 as an essential regulator of the actin cytoskeleton, leading us to examine its function in neutrophils during polarization and chemotaxis. We used neutrophil-like differentiated HL-60 (dHL-60) cells, which recapitulate the chemotactic responses of primary blood neutrophils. Unlike primary neutrophils, which are short lived in culture and refractory to genetic manipulations, HL-60 cells can be continuously cultured and are genetically tractable and therefore have been widely used for the study of neutrophil chemotaxis (Servant *et al.*, 2000; Hauert *et al.*, 2002; Srinivasan *et al.*, 2003; Xu *et al.*, 2003; Gomez-Mouton *et al.*, 2004; Bodin and Welch, 2005; Schymeinsky *et al.*, 2006; Weiner *et al.*, 2006; Nuzzi *et al.*, 2007; Neel *et al.*, 2009).

We assessed the expression of mTOR, Rictor, and Raptor in neutrophils. Undifferentiated HL-60 cells (uHL-60), dHL-60, and primary human neutrophils expressed mTOR, Raptor, and Rictor (Supplemental Figure S1A). Raptor is the major component of the mTORC1 (Wullschleger *et al.*, 2006; Bhaskar and Hay, 2007). Immunofluorescence of Rictor in nonstimulated dHL-60 cells was diffusely distributed, with some cortical localization around the plasma membranes, but was preferentially distributed to the leading edge of 71% of cells (of 126 examined) treated with the bacteria-derived chemoattractant formyl-Met-Leu-Phe (fMLP), colocalizing with F-actin (Figure 1A and data not shown). The immunofluorescence was specific for Rictor, as verified by competition experiments with a blocking peptide (Figure 1A; bottom). The asymmetric accumulation of Rictor was confirmed by quantitative analysis of fluorescence intensity across the cell, revealing a steep gradient of fluorescence signals (86 ± 15% decrease; Figure 1B). Moreover, the ratio of mean intensity of Rictor immunofluorescence between the leading and the trailing edges was 1.89 ± 0.09 (mean ± SEM; Figure 1C). By contrast, the ratio for green fluorescence protein (GFP) in polarized dHL-60 cells was 1.12 ± 0.11 (Figure 1C), indicating that the asymmetric distribution of Rictor was not due to overall morphological changes during neutrophil polarization.

mTOR and Rictor, but not mSin1, are required for neutrophil polarization and chemotaxis

Rictor's subcellular localization in polarized neutrophils suggested a potential role in controlling leading-edge protrusion and chemotaxis. To test this possibility, we used a lentivirus-based system to stably express small hairpin RNAs (shRNAs) that efficiently depleted mTOR, Rictor, and Raptor in dHL-60 cells (Figure 2, A and B). To ensure specificity, we used at least two shRNAs that deplete the same target genes. The chemotactic behaviors of mTOR-, Raptor-, or Rictor-depleted cells were examined by using a microfluidic gradient device, which enabled us to watch populations of cells moving in a highly stable gradient over a long distance (Herzmark *et al.*, 2007; He *et al.*, 2011). In this assay, cells containing nontarget (NT) shRNA polarized and moved rapidly in a concentration gradient of fMLP (1.4 nM/μm; Figure 2, C and D, Supplemental Figure S1B, and Supplemental Movie S1), as described earlier (He *et al.*, 2011). Of interest, depletion of Raptor or treatment with rapamycin, a potent and specific inhibitor for mTORC1, had little effect on cell polarization and migration, suggesting that mTORC1 is dispensable for neutrophil chemotaxis (Figure 2C and Supplemental Figure S1B). By contrast, cells with mTOR or Rictor depletion exhibited severe chemotactic defects (Figure 2, C and D, Supplemental Figure S1B, and Supplemental Movies S2 and S3). These cells failed to polarize properly and instead formed small, poorly developed and unstable leading edges (Figure 2, C and D, Supplemental Figure S1B, and Supplemental Movies S2 and S3). Only 9% of Rictor-depleted cells exhibited stable and persistent polarity during migration, in sharp contrast to control cells (89%). Furthermore, Rictor-depleted cells migrated much more slowly (Figure 2, C and D, and Supplemental Figure S1B), resulting in a large fraction of cells in the lower end of the fMLP gradient (Figure 2C). In addition, the chemotactic indices, defined as the ratio of migration in the correct direction to the actual length of the migration path (Xu *et al.*, 2005; He *et al.*, 2011), were 0.81 and 0.63 for control and Rictor-depleted cells, respectively, suggesting defects in directional migration upon Rictor depletion (data not shown). The chemotactic behaviors of mTOR and Rictor-depleted cells were also examined by using the micropipette chemotaxis assay. In this assay, mTOR- or Rictor-depleted cells showed polarization and migration defects highly reminiscent of those in the microfluidic assay (Supplemental Figure S1C; see Supplemental Movies S4 and S5, which show the migratory behaviors of

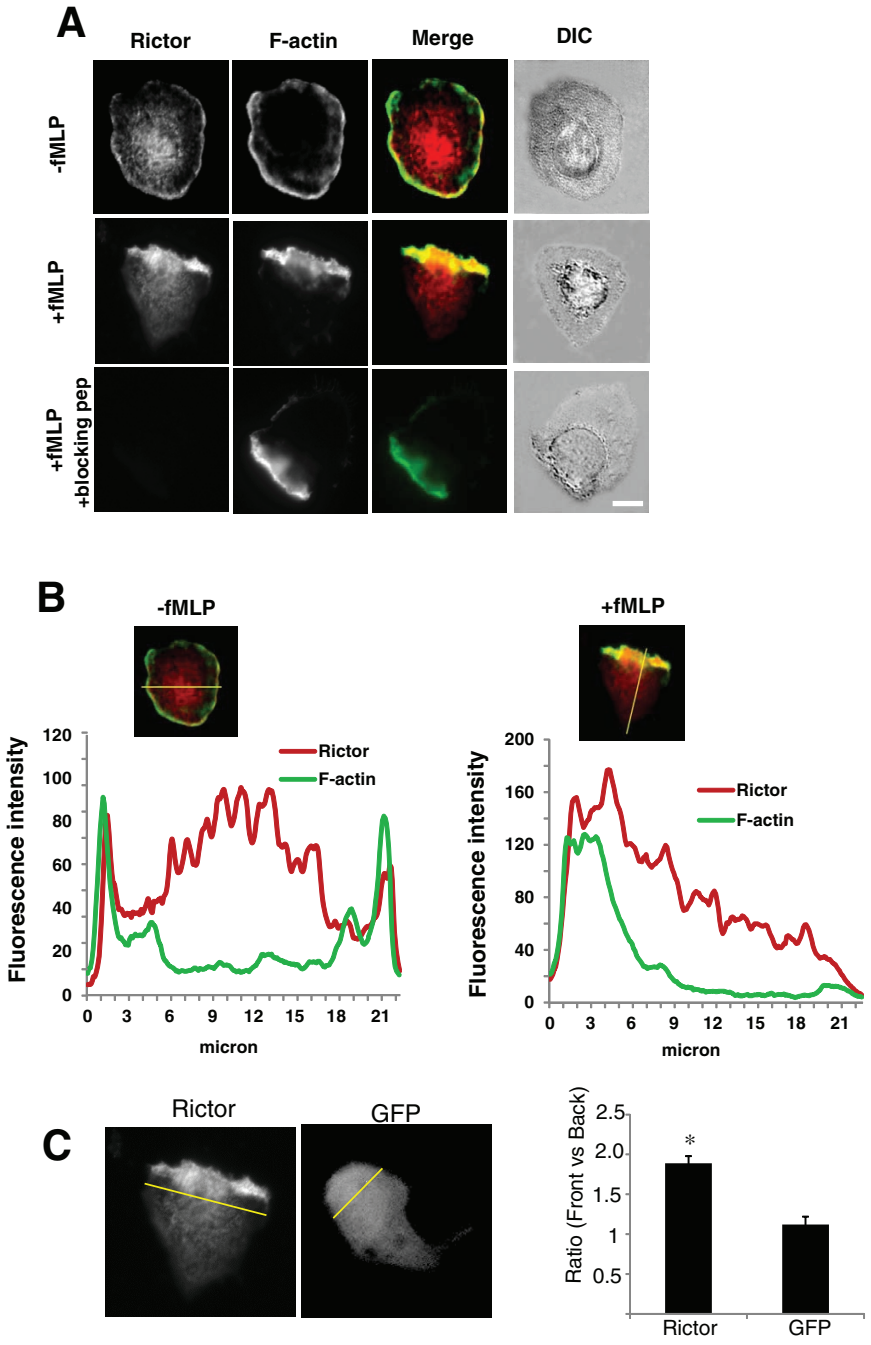

FIGURE 1: Rictor is recruited to the leading edge of polarized dHL-60 cells. (A) Immunofluorescence of Rictor (red) and F-actin (green) in cells plated on fibrinogen without (top) or with (middle) fMLP stimulation (100 nM, 2 min). Fluorescence images of Rictor (red), F-actin (green), Rictor/F-actin merged images, and differential interference contrast (DIC) images of cells. The Rictor immunofluorescence is specific because incubation with the Rictor peptide completely abolishes the immunofluorescence (bottom). Bar, 10 μm. (B) Fluorescence line profiles of Rictor (Red) and F-actin (green) in dHL-60 cells with or without fMLP stimulation. The graph below the fluorescence image plots the fluorescence intensity of each probe (*y*-axis) vs. distance (*x*-axis) for the corresponding cell. (C) Ratios of mean fluorescence intensity of Rictor and GFP between the front and the back of cells. Left, representative Rictor and GFP images; right, quantification of 41 cells (for Rictor) and 38 cells (for GFP) collected from four independent experiments. The front of the cell is defined as the area within the first 3 μm of the cell (indicated by the yellow line), as depicted earlier (Shin *et al.*, 2010), and the rest of the cell is defined as the back. Student's *t* test was performed. The asterisk indicates that the ratio for Rictor differs statistically from that of GFP (*$p < 0.01$).

cells in gradients created by the micropipette). To further examine the specificity of Rictor depletion, we ectopically expressed wild-type Rictor in dHL-60 cells with Rictor depleted (Figure 2E). We used shRNAs targeting 3′-untranslated region (UTR) of Rictor, which specifically deplete endogenous Rictor, not the ectopic form. The endogenous gene products were depleted, whereas the exogenously expressed mRNAs devoid of the 3′-UTR were resistant. The ectopic expression of wild-type Rictor largely rescued the polarization and migratory defects caused by Rictor depletion (Figure 2, F and G, and data not shown). Taken together, these results suggest that mTOR and Rictor, but not Raptor, are required for neutrophil chemotaxis.

mTOR has a well-documented role in the regulation of cell growth, survival, and differentiation (Sarbassov *et al.*, 2005a; Wullschleger *et al.*, 2006; Bhaskar and Hay, 2007). We asked whether the migratory defect in cells with mTOR or Rictor depletion might be attributed to compromised cell survival and differentiation. We found that Rictor-depleted cells exhibited a similar rate of apoptosis (3.0 ± 1.4%) to the control cells (1.8 ± 0.7%), whereas mTOR depletion slightly increased apoptosis (6.0 ± 2.4%) (Supplemental Figure S1D). In addition, Rictor depletion did not alter the level of β2 integrin, a marker for neutrophil differentiation (Supplemental Figure S1E). Of interest, mTOR depletion significantly reduced the level of β2 integrin (Supplemental Figure S1E). Furthermore, when exposed to fMLP, cells with Rictor depletion showed similar levels of intracellular calcium release to the control cells (Supplemental Figure S1F). Finally, Rictor depletion did not alter fMLP-induced phosphorylation of AKT (at threonine 308; see the rest of this study; Supplemental Figure S2A), again demonstrating that Rictor depletion does not nonspecifically perturb the function of neutrophils. The differential effect of mTOR depletion on β2 integrin expression is probably mediated by mTORC2/Rictor–independent signals and/or other mechanisms.

To further test the potential role of mTORC2 in controlling leading-edge protrusion and chemotaxis, we depleted mSin1, an indispensable component of mTORC2 necessary for AKT phosphorylation at serine 473 (S473; Frias *et al.*, 2006; Jacinto *et al.*, 2006; Yang *et al.*, 2006), using two separate shRNAs (Supplemental Figure S2B). Surprisingly, whereas the shRNAs substantially reduced the levels of mSin1 in dHL-60 cells (Supplemental Figure S2B), we failed to

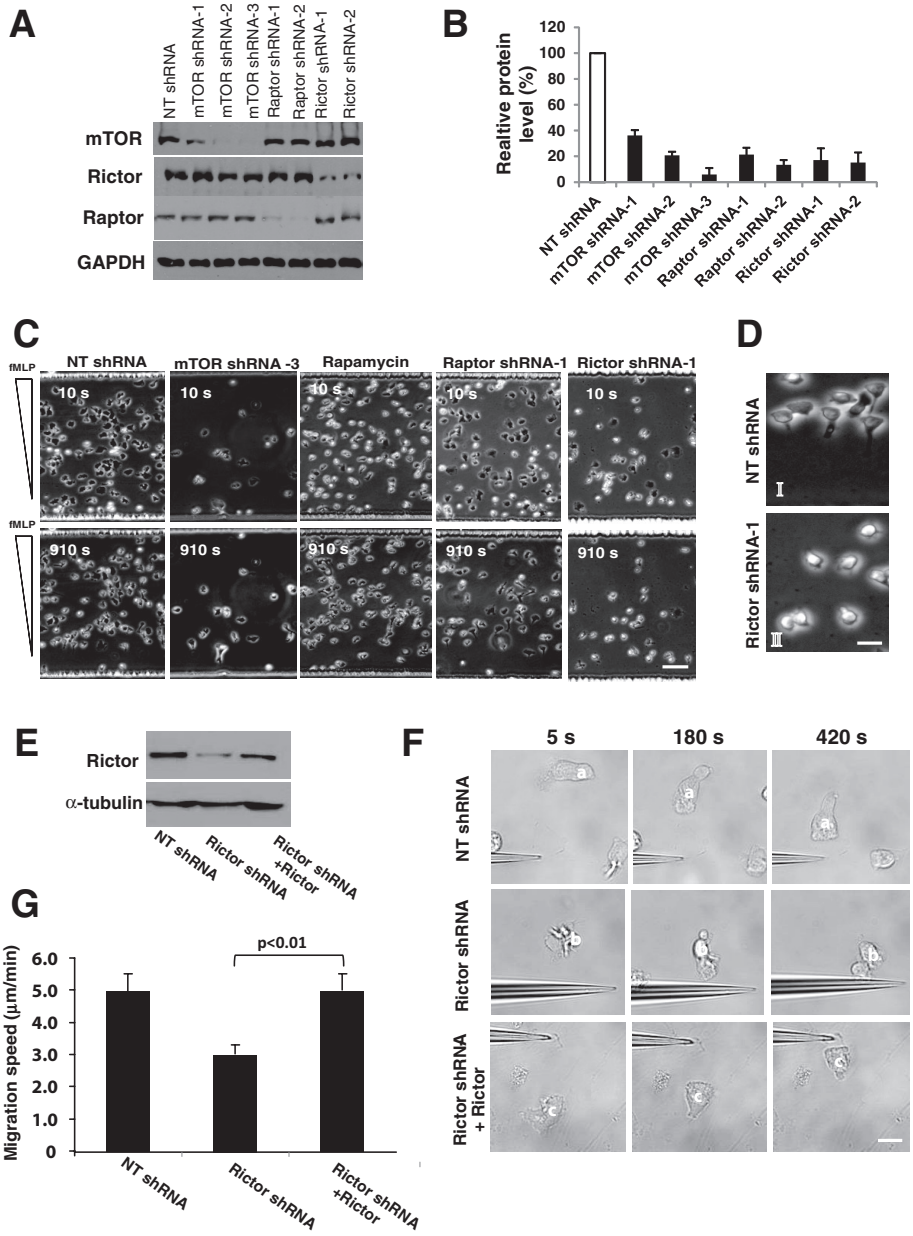

FIGURE 2: Rictor depletion impairs dHL-60 chemotaxis. (A) Western blotting of mTOR, Raptor, and Rictor in dHL-60 cells transfected with specific or NT shRNAs. GAPDH was a loading control. HL-60 cells were infected with lentiviruses containing the various shRNAs and were differentiated for 5 d in the presence of DMSO. (B) Relative levels of mTOR, Raptor, and Rictor in cells with or without depletion. Values are normalized to the level in control cells (with the NT shRNA, 100%) and are means ± SEM ($n = 4$). (C) Chemotaxis of dHL-60 cells with various treatments in a microfluidic gradient device. After adhering to the fibrinogen-coated surface of the microfluidic chamber, cells (2×10^6) were exposed to an fMLP gradient for 20 min. Phase-contrast images of cells 10 and 910 s after fMLP stimulation. Bar, 50 μm. Supplemental Movies S1–S3 are of cells with or without mTOR and Rictor depletion. (D) Images with higher magnification of cells with NT (I) and Rictor shRNA (II) treatment, 910 s after exposure to fMLP gradients. Bar, 10 μm. (E) Western blotting of Rictor in control and Rictor-depleted dHL-60 cells with or without rescue. Rictor-depleted cells were differentiated and transfected with wild-type (WT) Rictor. α-Tubulin was a loading control. (F) Wild-type Rictor rescues the migratory defects of Rictor-depleted cells revealed with the micropipette assay. Time-lapse images of representative cells for various conditions. The three images in each column show the positions of individual cells (identified with a superimposed letter) after exposure to fMLP. Bar, 10 μm. (G) Speeds of cell migration for control, Rictor-depleted, and rescued cells revealed with the micropipette assay. Values are means ± SEM ($n = 21$ for control, 16 for Rictor shRNA alone, and 15 for Rictor shRNA plus wild-type Rictor). The cells with Rictor rescue differ statistically from the Rictor-depleted cells ($p < 0.01$).

detect chemotactic defects in mSin1-depleted cells: these cells migrated with similar degree of polarization (81 and 82% of polarized cells for mSin1 shRNA1 and shRNA 2, respectively) and migration speeds (3.4 and 3.0 μm/min for shRNA1 and shRNA2, respectively) comparable to cells with NT shRNAs (89% and 2.8 μm/min, respectively; Supplemental Figure S2C and data not shown). Furthermore, mSin1 depletion robustly decreased the level of S473-phosphorylated AKT (pS473-AKT) in cells stimulated with fMLP (Supplemental Figure S2D), indicating that the depletion effectively impairs downstream signaling activities. Because Rictor, but not mSin1, is required for neutrophil polarity and migration, our findings suggest that Rictor regulates neutrophil chemotaxis in an mTORC2-independent manner.

mTORC2-mediated AKT phosphorylation is not required for neutrophils chemotaxis

The kinase activity of mTOR is responsible for S473 phosphorylation of AKT in cells exposed to nutrient signals (Sarbassov *et al.*, 2005b). In budding yeast, TorC2 regulates actin polymerization through the ACG kinase YPK2, the yeast AKT homologue (Schmidt *et al.*, 1996; Kamada *et al.*, 2005). Similarly, TORC2 in *D. discoideum* activates PKBR1 and PKBA, the AKT homologues in *D. discoideum*, which in turn regulate polarity and chemotaxis (Lee *et al.*, 2005; Kamimura *et al.*, 2008). These results led us to examine whether AKT might mediate Rictor's response in neutrophils during chemotaxis.

We first assessed the level of S473-phosphorylated AKT in control and Rictor-depleted cells. Exposure of control dHL-60 cells to fMLP induced rapid and robust phosphorylation of AKT, reaching a maximum at 60 s (Supplemental Figure S3, A and B), in keeping with earlier reports (Wang *et al.*, 2002; He *et al.*, 2011). Rictor depletion markedly reduced S473-phosphorylation of AKT (to 12.4 ± 8.2% of control cells; Supplemental Figure S3, C–D). In contrast, threonine 308 (T308) phosphorylation of AKT, which was reportedly catalyzed by PDK1 (Alessi *et al.*, 1997; Belham *et al.*, 1999), was unaltered in Rictor-depleted cells (Supplemental Figure S2A). These data suggested that Rictor is a key regulator of AKT S473 phosphorylation in dHL-60 cells exposed to fMLP.

We next asked whether inhibition of AKT phosphorylation impaired chemotaxis. We used a specific AKT inhibitor, AKTi-1/2, which abolishes AKT phosphorylation at

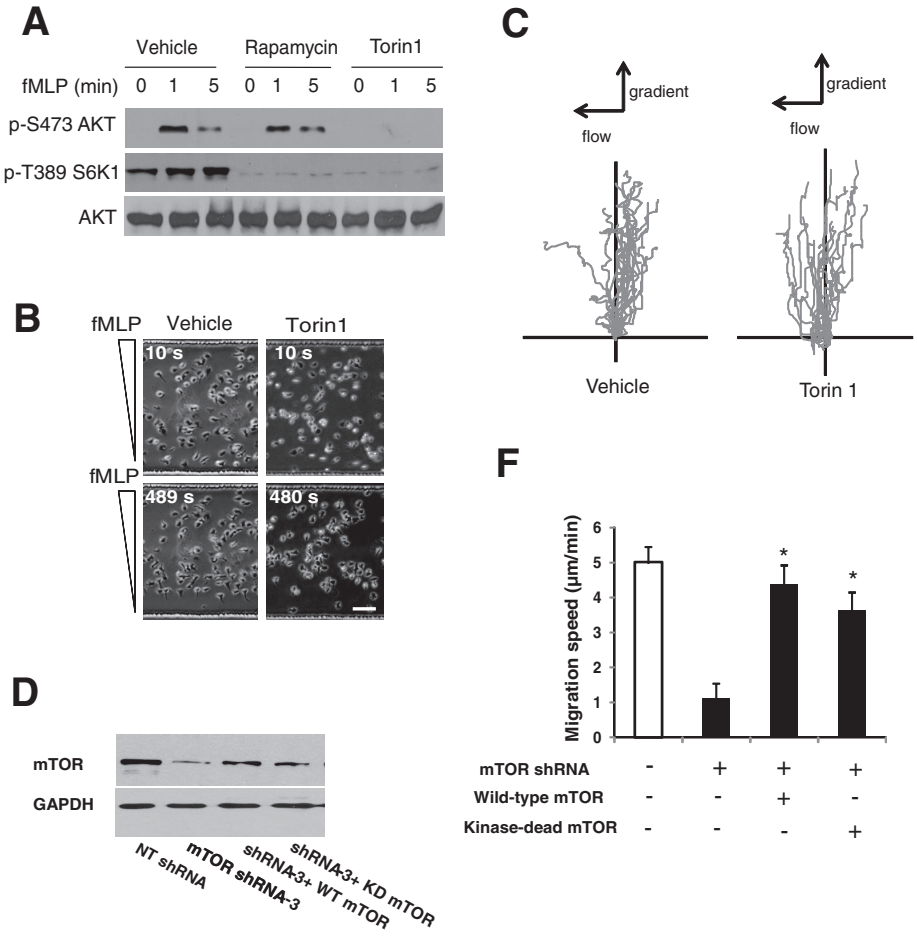

FIGURE 3: mTOR kinase activity is dispensable for chemotaxis. (A) Western blotting of AKT (p-S473) and S6K1 (p-T389) phosphorylation in cells pretreated with vehicle (DMSO), rapamycin (100 nM), or Torin1 (250 nM) for 30 min and stimulated with fMLP (100 nM) for indicated time points. AKT is the loading control. (B) Chemotaxis of dHL-60 cells with or without Torin1 treatment (250 nM, 30 min) in a microfluidic gradient device. Phase-contrast images of cells 10 and 480 s after fMLP stimulation. Bar, 50 μm. (C) Trajectory of dHL-60 cells migrating in the microfluidic chamber. Cell migration was recorded using time-lapse microscope, and the migration path of individual cells was analyzed and plotted using ImageJ (National Institutes of Health, Bethesda, MD). (D) Western blotting of mTOR in control and mTOR-depleted dHL-60 cells with or without rescue. mTOR-depleted cells were differentiated and transfected with WT mTOR or a kinase-dead mutant of mTOR. mTOR was depleted with shRNA-3, which targets the 3′-UTR of mTOR and thus exerts no effect on ectopically expressed mTOR. GAPDH is the loading control. (E) Both wild-type mTOR and the kinase-dead mTOR mutant rescue the migratory defects of mTOR-depleted cells revealed with the micropipette assay. Time-lapse images of representative cells for various conditions. The two images in each column show the positions of individual cells (identified with a superimposed letter) after exposure to fMLP. Bar, 10 μm. (F) Speeds of cell migration for control, mTOR-depleted, and rescued cells revealed with the micropipette assay. Values are means ± SEM ($n = 18$ for control, 19 for mTOR shRNA alone, 17 for mTOR shRNA plus wild-type mTOR, and 15 for mTOR shRNA plus mTOR kinase-dead mutant). Asterisks indicate that the cells differ statistically from the mTOR-depleted cells (*$p < 0.001$).

both S473 and T308 in vitro and in vivo (Barnett *et al.*, 2005). This inhibitor potently inhibited AKT phosphorylation in dHL-60 cells and human primary neutrophils (Supplemental Figure S3E) but failed to affect chemotaxis in experiments with both the microfluidic (Supplemental Figure S3, F and G) and the micropipette assays (data not shown). The AKTi-1/2–treated cells polarized and migrated similarly to control cells and exhibited similar chemotactic index (0.87 and 0.86, respectively; Supplemental Figure S3, F and G, and data not shown). These data indicate that AKT phosphorylation is not responsible for Rictor's function in neutrophil polarization and chemotaxis.

mTOR kinase activity is dispensable for chemotaxis

The lack of function for AKT phosphorylation in chemotaxis led us to ask whether mTOR kinase activity was required for neutrophil polarization and chemotaxis. An ATP analogue inhibitor of mTOR kinase, Torin1, was developed and reportedly inhibits mTORC1 and mTORC2 kinase activities in a variety of cells (Thoreen *et al.*, 2009). We assessed the effect of Torin1 on neutrophil chemotaxis.

We found that Torin1 treatment markedly reduced the levels of both phosphorylated S6K1 (at threonine 389) and AKT (by 84 and 88%, respectively; Figure 3A and Supplemental Figure S4, A and B). By contrast, rapamycin treatment reduced S6K1 phosphorylation by 79% but had little effect on AKT phosphorylation (Figure 3A and Supplemental Figure S4, A and B). Despite its ability to inhibit S6K1 and AKT phosphorylation, Torin1 treatment had no detectable effects on chemotaxis of dHL-60 cells and primary neutrophils (Figure 3, B and C, Table 1, and data not shown).

To further determine whether the kinase activity of mTOR was required for chemotaxis, we ectopically expressed wild-type mTOR and the kinase-dead mutant (Asp2357-Glu; Vilella-Bach *et al.*, 1999) in dHL-60 cells with endogenous mTOR depleted (Figure 3D). As shown in Figure 3, E and 3F, expression of either

Cells	Parameter	DMSO	Rapamycin	Torin1
dHL-60	Speed (μm/min)	4.36 ± 0.16	4.39 ± 0.12	4.67 ± 0.13
	Chemotactic index	0.97 ± 0.01	0.95 ± 0.01	0.96 ± 0.01
Primary neutrophil	Speed (μm/min)	7.05 ± 0.12	7.40 ± 0.55	7.47 ± 0.21
	Chemotactic index	0.96 ± 0.01	0.97 ± 0.01	0.96 ± 0.01

Cells were pretreated with DMSO, Torin1 (250 nM, 30 min), and rapamycin (100 nM, 30 min) before chemotaxis assay. The chemotactic index is defined as the ratio of migration in the correct direction to the actual length of the migration path (Xu *et al.*, 2005).

TABLE 1: Effects of drug inhibition on dHL-60 cell and primary neutrophil chemotaxis.

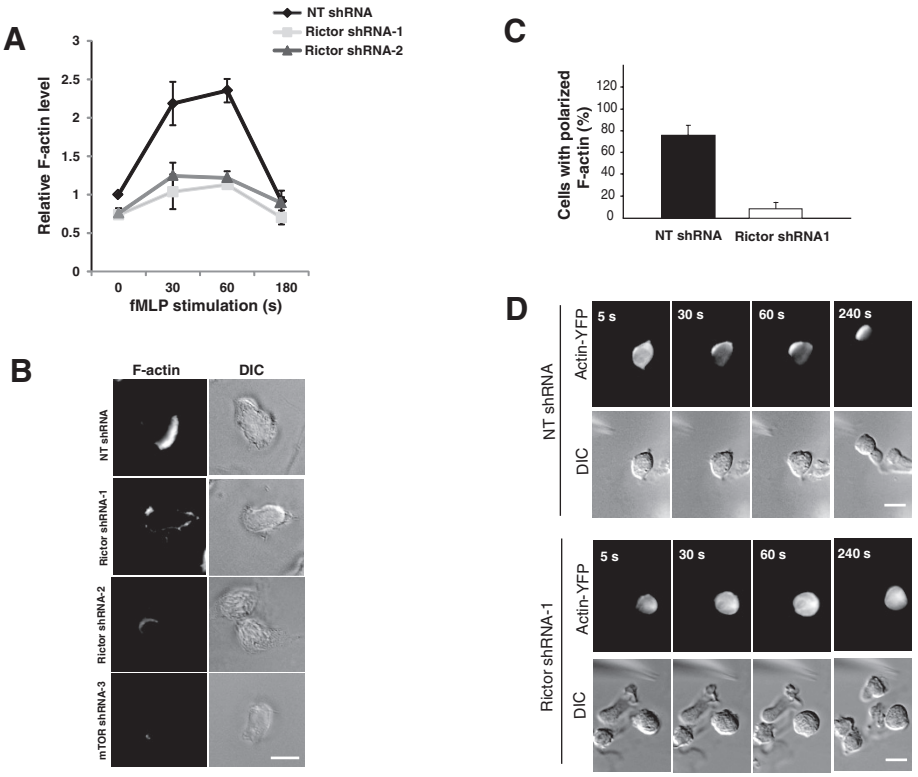

FIGURE 4: Rictor depletion impairs actin polymerization in dHL-60 cells. (A) Quantification of F-actin levels in suspended cells. Cells with or without Rictor depletion were stimulated with fMLP (100 nM) for various times in suspension and fixed for staining with fluorescently labeled phalloidin. Fluorescence in stained cells was determined by flow cytometry. Values are mean ± SEM ($n = 4$). (B) F-actin staining of dHL-60 cells with or without Rictor or mTOR depletion after fMLP stimulation. Cells were plated on fibrinogen-coated coverslips for 20 min and stimulated with uniform fMLP (100 nM) for 2 min. Images of F-actin and DIC. Bar, 10 μm. (C) Quantification of the number of dHL-60 cells with polarized actin polymerization with and without Rictor depletion. Cells were stimulated with uniform fMLP (100 nM) for 2 min, as described in B. Each bar represents the mean ± SEM ($n = 4$). (D) The dynamics of actin-YFP in dHL-60 cells exposed to an fMLP gradient. HL-60 cells stably expressing actin-YFP were infected with lentivirus containing NT shRNA or Rictor shRNA (shRNA-1) and subsequently differentiated for 5 d. Cells were plated on fibrinogen-coated coverslips and stimulated with a chemotactic gradient delivered by a micropipette containing 10 μM fMLP for the times indicated. Fluorescence images of actin-YFP and the corresponding DIC images. Bar, 10 μm.

wild-type mTOR or the kinase-dead mTOR mutant largely rescued the chemotactic defects caused by mTOR depletion. To specifically deplete endogenous mTOR, not the ectopic form, we used shRNAs targeting 3′-UTR of mTOR. Together these data indicate that mTOR kinase activity is dispensable for neutrophil chemotaxis.

mTOR and Rictor regulate assembly of the actin cytoskeleton in neutrophils

How might Rictor control neutrophil polarization and chemotaxis? The emerging role of TORC2/Rictor in regulating the actin cytoskeleton in several cell types (Schmidt *et al.*, 1996; Jacinto *et al.*, 2004; Sarbassov *et al.*, 2004; Wullschleger *et al.*, 2006), asymmetric localization of Rictor at the leading edge of neutrophils (Figure 1), and the effect of Rictor depletion on neutrophil leading-edge establishment and polarization (Figure 2) led us to ask whether Rictor regulates fMLP-induced actin skeleton assembly in neutrophils during chemotaxis.

We measured the level of F-actin in both suspended and adherent cells with or without Rictor depletion (Figure 4). As described previously (Wang *et al.*, 2002; Weiner *et al.*, 2006; Shin *et al.*, 2010), exposure of suspended control dHL-60 cells (i.e., containing NT shRNAs) induced rapid and transient actin polymerization, which peaked at around 1 min (Figure 4A). Rictor depletion moderately reduced the level of F-actin in cells under resting conditions (by ~20%) and substantially abolished the transient accumulation of F-actin in suspended cells after exposure to chemoattractant (Figure 4A). Similarly, mTOR depletion also substantially decreased the level of actin polymerization in suspended dHL-60 cells (Supplemental Figure S5A). In addition, when plated on the fibrinogen substrate and exposed to a uniform concentration of fMLP, control cells developed a polarized morphology with F-actin concentrated at the leading edge, as revealed by phalloidin staining (Figure 4B, top). Rictor depletion in the adherent cells nearly completely prevented polarized morphology and F-actin accumulation (Figure 4B). Quantitative analysis revealed that only 12% of Rictor-depleted cells showed asymmetric accumulation of F-actin at the leading edge, in sharp contrast to control cells (78%; Figure 4C). Similar to Rictor depletion, mTOR depletion markedly impaired F-actin accumulation in adherent cells, in keeping with its effect on cell polarization and migration (Figure 4B).

To document the response of actin throughout fMLP stimulation, we assessed the effect of Rictor depletion in live cells. We delivered

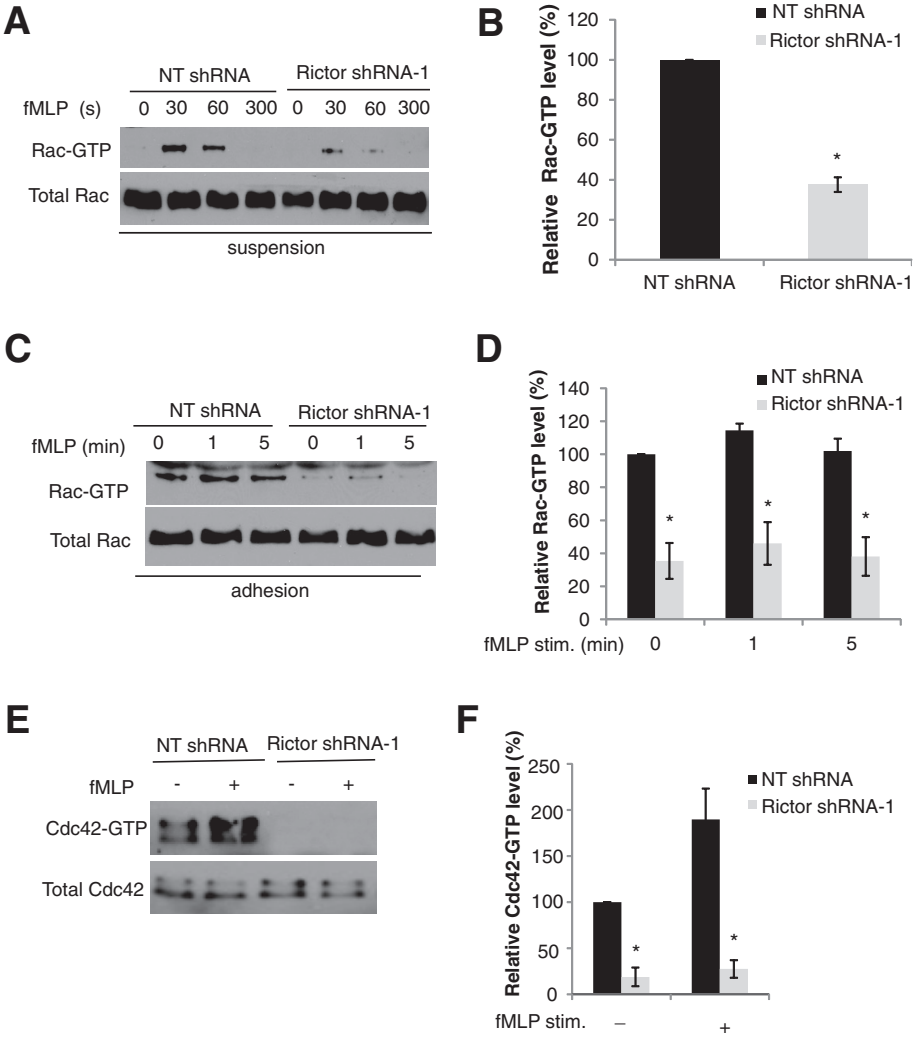

FIGURE 5: Rictor depletion impairs Rac and Cdc42 activities in dHL-60 cells. (A) The levels of Rac-GTP in suspended dHL-60 cells. dHL-60 cells with or without Rictor depletion were stimulated with 100 nM of fMLP for various time points in suspension and lysed for the pull-down assay. Levels of total Rac were used to show cell lysate input. (B) Quantification of relative levels of Rac-GTP level in suspended dHL-60 cells with and without Rictor depletion 30 s after fMLP stimulation. Each bar represents the mean ± SEM (error bars). Values are normalized to the level of Rac-GTP (= 100%) in cells without Rictor depletion (*$p < 0.001$). (C) The levels of Rac-GTP in adherent dHL-60 cells. Control cells or Rictor-depleted cells plated on fibrinogen-coated plates were unstimulated or stimulated for 1 or 5 min with a uniform concentration of fMLP (100 nM) and lysed for pull-down assay. Levels of total Rac were used to show cell lysate input. (D) Quantification of relative levels of Rac-GTP in adherent dHL-60 cells with and without Rictor depletion. Each bar represents the mean ± SEM ($n = 4$). Values are normalized to the level of Rac-GTP (= 100%) in cells without Rictor depletion before fMLP stimulation (*$p < 0.001$). (E) The levels of Cdc42-GTP in dHL-60 cells with or without Rictor depletion. dHL-60 cells with or without Rictor depletion were stimulated with 100 nM of fMLP for 30 s in suspension and lysed for the pull-down assay. Levels of total Cdc42 were used to show cell lysate input. (F) Quantification of relative levels of Cdc42-GTP in suspended dHL-60 cells with and without Rictor depletion. Each bar represents the mean ± SEM ($n = 4$). Values are normalized to the level of Cdc42-GTP (= 100%) in cells without Rictor depletion before fMLP stimulation (*$p < 0.001$).

NT shRNA or Rictor-specific shRNAs into dHL-60 cells stably expressing actin–yellow fluorescent protein (YFP; Shin *et al.*, 2010) and stimulated the cells with a point source of fMLP. As shown earlier (Shin *et al.*, 2010), control cells responded to fMLP stimulation by translocating actin-YFP from the cytosol to the cell's leading edge (Figure 4D). By contrast, in Rictor-depleted cells actin-YFP remained diffusely distributed through the entire course of fMLP stimulation (Figure 4D). Only 1 of 14 Rictor-depleted cells showed actin accumulation, in contrast to control cells (16 of 18).

We next asked whether Rictor depletion also influenced the level of F-actin in neutrophil-like PLB-985 cells. Two shRNAs effectively depleted Rictor in differentiated PLB-985 (dPLB-985) cells, consistent with their effects in dHL-60 cells (Supplemental Figure S5B). Rictor depletion markedly reduced the migration speed of dPLB-985 cells and the level of actin polymers in response to fMLP stimulation (Supplemental Figure S5, C and D, and data not shown). These effects were similar to those in dHL-60 cells. Together our findings suggest that Rictor acts to control assembly of the actin cytoskeleton in neutrophils during chemotaxis.

Depletion of Rictor inhibits Rac and Cdc42 activities

If AKT does not mediate Rictor's function in neutrophils, how might Rictor regulate actin polymerization and organization during neutrophil chemotaxis? Rac and Cdc42 are members of the Rho GTPase family, which have well established roles in the regulation of actin dynamics in various cell types (Sanchez-Madrid and del Pozo, 1999; Etienne-Manneville and Hall, 2002). Rac2 deletion in mouse neutrophils or expression of dominant-negative Rac mutants in human neutrophil cell lines markedly prevents cell polarization and actin polymerization (Roberts *et al.*, 1999; Williams *et al.*, 2000; Srinivasan *et al.*, 2003). Inhibition of Cdc42 in neutrophils with dominant-negative mutants impairs leading-edge stability and persistent motility (Srinivasan *et al.*, 2003). We therefore asked whether Rac and/or Cdc42 might serve as downstream targets to mediate the function of Rictor in neutrophils (Figure 5).

We first assessed the level of Rac-GTP using a previously described pull-down method (Benard *et al.*, 1999) in suspended dHL-60 cells. When in suspension, cells are free of other signaling input and provide a better understanding of chemoattractant-induced signaling activities. Under these conditions, the level of Rac-GTP increased rapidly and transiently after exposure to fMLP, reaching a maximum at 30 s (Figure 5A), in keeping with earlier reports (Benard *et al.*, 1999; Xu *et al.*, 2003; Van Keymeulen *et al.*, 2006). Rictor depletion reduced the level of Rac-GTP by >60% (37.6 ± 3.7% of control; Figure 5, A and B). The inhibitory effect of Rictor depletion on Rac activity was also observed in cells adhered to the fibrinogen-coated substrate (Figure 5, C and D). Of note, in adherent cells Rictor depletion reduced the level of active Rac not only in cells stimulated with fMLP, but also in those without fMLP stimulation (Figure 5, C and D).

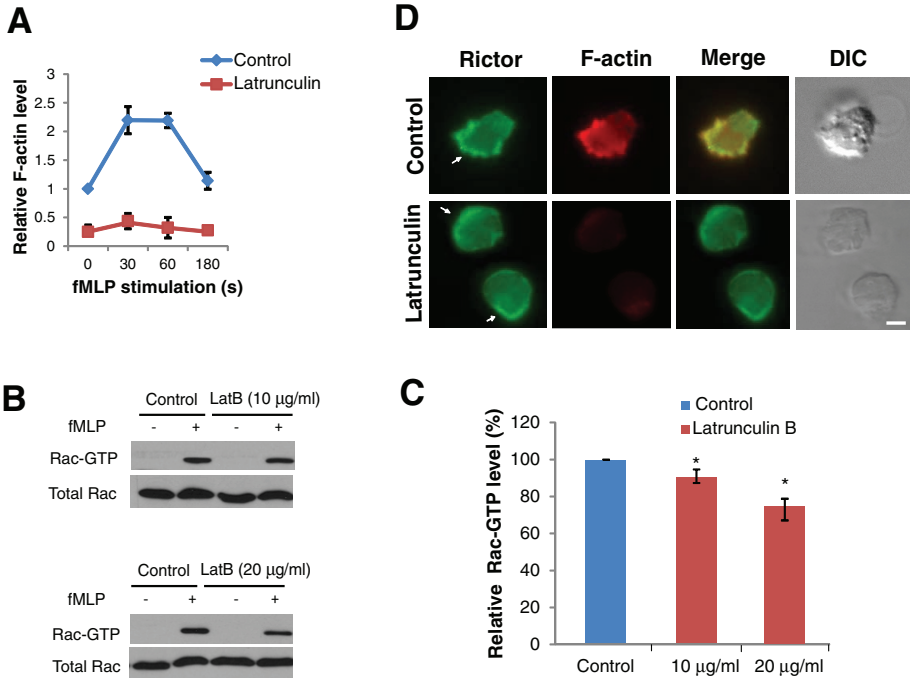

FIGURE 6: Actin polymers are not responsible for Rictor regulation of Rac activity. (A) Quantification of F-actin levels in suspended cells. Cells with or without pretreatment of latrunculin B (10 µg/ml, 10 min) were stimulated with fMLP (100 nM) for various times in suspension and fixed for staining with fluorescently labeled phalloidin. (B) The levels of Rac-GTP in suspended dHL-60 cells with or without latrunculin B pretreatment (10 min; 10 µg/ml, top; 20 µg/ml, bottom) were stimulated with 100 nM of fMLP (30 s) and lysed for the pull-down assay. Levels of total Rac were used to show cell lysate input. (C) Quantification of relative levels of Rac-GTP level in suspended dHL-60 cells with or without latrunculin B pretreatment 30 s after fMLP stimulation. Each bar represents the mean ± SEM (error bars). Values are normalized to the level of Rac-GTP (= 100%) in cells without latrunculin B pretreatment (*$p < 0.001$). (D) The fluorescence image of Rictor (green), F-actin (red), and merged Rictor and F-actin image and DIC image of dHL-60 cells pretreated or not pretreated with latrunculin B (10 µg/ml, 10 min) and stimulated with a uniform concentration of fMLP (100 nM, 1 min). The white arrows point to the areas with Rictor cortical localization. Bar, 10 µm.

Furthermore, Rictor depletion substantially reduced the activity of Cdc42 in dHL-60 cells (Figure 5, E and F). Similar to Rictor depletion, depletion of mTOR also decreased the levels of active Rac and Cdc42 in fMLP-stimulated cells (Supplemental Figure S6). Therefore Rac and Cdc42 might function as key effectors of Rictor to mediate actin polymerization and organization in neutrophils during chemotaxis. The relatively high level of Rac activity in adherent cells before fMLP stimulation probably resulted from cell adhesion to the extracellular matrix (ECM) substrate; it is well known that integrin–ECM ligation can induce Rac activation (Price *et al.*, 1998).

Liu *et al.* (2010) reported that in differentiated PLB-985 cells mTORC2 primarily controls myosin II activity through a cAMP/RhoA-signaling axis. These findings prompted us to evaluate whether Rictor depletion in dHL-60 cells also affected Rho activities. In suspended cells, Rictor depletion in dHL-60 cells led to increased Rho activation only after prolonged fMLP stimulation (Supplemental Figure S7A). In adherent cells, however, no significant difference in RhoA activity was observed between control and Rictor-depleted cells (Supplemental Figure S7B). These results suggest that the RhoA signaling pathway is probably not the main target of Rictor in dHL-60 cells.

Rho-GDP dissociation inhibitor (RhoGDI) functions as an inhibitor of the Rho family proteins. It was recently reported that Rictor regulates migration of mouse embryonic fibroblasts by suppressing the level of RhoGDI2 (Agarwal *et al.*, 2013). Depletion of Rictor in these cells thereby leads to increased RhoGDI2 levels, which consequently decrease the activity of Rac and Cdc42. To investigate whether Rictor also modulates RhoGDI2 in dHL-60 cells, we assessed the protein level of RhoGDI in Rictor-depleted cells. We did not observe alterations in RhoGDI2 protein levels upon Rictor depletion (Supplemental Figure S7C). Thus it is unlikely that RhoGDI2 is involved in Rictor regulation of Rac and Cdc42 activities in neutrophils.

Actin polymers are not responsible for Rictor regulation of Rac activity

It was demonstrated that actin polymers serve as a component of a feedback loop containing PI(3,4,5)P3 and Rac (Xu *et al.*, 2003) in chemotaxing neutrophils and that inhibition of actin polymerization impairs chemoattractant-induced Rac activation (Van Keymeulen *et al.*, 2006). Because Rictor depletion markedly reduced the level of actin polymers (Figure 4A), these findings raise the possibility that Rictor might regulate Rac activity via actin polymerization. To test this, we treated dHL-60 cells with latrunculin B, a widely used inhibitor of actin polymerization, and assessed the effect on fMLP-induced Rac activation (Figure 6, A–C). As shown in Figure 6, B and 6C, treatment of cells with an intermediate concentration of latrunculin B (10 µg/ml, 10-min pretreatment) slightly reduced fMLP-induced Rac activation (~9% reduction compared with control cells), whereas a higher latrunculin B concentration (20 µg/ml) caused a stronger effect (~26% reduction). Of note, even at the concentration of 10 µg/ml, latrunculin B had a stronger inhibitory effect on actin polymerization than Rictor depletion (Figure 6A; compare with Figure 4A). Because Rictor depletion led to >60% reduction in Rac-GTP (Figure 5, A and B), the decrease in actin polymerization alone cannot account for Rictor's effect on Rac activities. Therefore actin polymerization might contribute to but is not responsible for Rictor regulation of Rac activities in neutrophils during chemotaxis.

In keeping with these results, although dHL-60 cells with latrunculin B pretreatment (10 µg/ml, 10 min) failed to polarize and exhibited little actin polymers to fMLP stimulation (Figure 6, A and D, bottom), they nevertheless exhibited prominent cortical localization of Rictor around the cell's periphery (Figure 6D). Of 54 cells examined, 39 (72%) exhibited accumulation of Rictor immunofluorescence in cortical areas of fMLP-stimulated cells. These findings suggest that Rictor likely acts upstream of actin assembly in the chemotactic signaling cascade in neutrophils.

DISCUSSION

In conclusion, our results reveal a critical role for mTOR and Rictor in the regulation of neutrophil chemotaxis. We found that depletion of mTOR and Rictor in neutrophil-like dHL-60 cells impairs leading-edge establishment, cell polarization, and directional migration.

Our data suggest that Rictor regulates neutrophil polarity and chemotaxis by primarily controlling the actin cytoskeleton assembly and organization at the neutrophil's leading edge. First, in response to chemoattractant, Rictor translocates to the leading edge of polarizing neutrophils, colocalizing with F-actin. Second, depletion of Rictor impairs chemoattractant-induced actin polymerization in both suspended and adherent cells. Finally, depletion of Rictor substantially reduces activities of Rac and Cdc42, both of which are essential regulators of actin dynamics and neutrophil chemotaxis. Our results confirm and extend previous findings in budding yeast, *D. discoideum*, 3T3 fibroblasts, and HeLa cells, demonstrating that Rictor is an essential regulator of the actin cytoskeleton in neutrophils during chemotaxis. In addition, we show, for the first time, that Rictor regulates neutrophil chemotaxis through mechanisms independent of mTORC2 and mTOR kinase activity.

How might mTOR and Rictor regulate the actin cytoskeleton in neutrophils? Intriguingly, our experiments show that depletion of mSin1, an integral component of mTORC2, causes no detectable defects in neutrophil polarization and migration, suggesting that Rictor functions through an mTORC2-independent mechanism(s). Our results are in keeping with a recent report, which demonstrated that Rictor controls migration of mouse embryonic fibroblasts (MEFs) in an mSin1-independent manner (Agarwal *et al.*, 2013). These authors, however, did not examine the function of mTOR in MEF migration. An mTORC2-independent function was also reported for Rictor in promoting SGK1 ubiquitination and destruction (Gao *et al.*, 2010). In addition, we found that mTOR kinase activity is dispensable for chemotaxis, and in keeping with the lack of kinase function, inhibition of AKT activity in neutrophils fails to affect cell polarization and chemotaxis, indicating that, unlike in *D. discoideum,* AKTs are not a major effector of Rictor in regulating chemotaxis. Instead, we show that Rictor depletion markedly reduces Rac and Cdc42 activities, similar to earlier studies using fibroblasts (Jacinto *et al.*, 2004; Agarwal *et al.*, 2013). Of interest, although inhibition of mTOR kinase activity has little effect, depletion of mTOR significantly impairs neutrophil polarity and migration, highly reminiscent of the defects caused by Rictor depletion. Whether mTOR interacts with Rictor to regulate neutrophil chemotaxis or these two molecules function independently remains to be defined.

Given the established roles of Rac and Cdc42 in the regulation of actin assembly and organization in neutrophils, it is likely that Rac and Cdc42, instead of RhoA, are the downstream targets that mediate Rictor's function during chemotaxis. First, the difference in RhoA activity between control and Rictor-depleted cells in suspension is very minimal at the early stage of fMLP stimulation (30 s; Supplemental Figure S7A), whereas the decrease in Rac/Cdc42 activity and F-actin is much more significant at this time point. Furthermore, Rictor depletion in adherent cells fails to reduce RhoA activity (Supplemental Figure S7B) but significantly decreases Rac activity throughout fMLP stimulation (Figure 5, C and D). Four possibilities, alone or in combination, could account for the actions of Rictor on Rac/Cdc42. It might be that Rictor carries its mTORC2-independent functions by binding to integrin-linked kinase (McDonald *et al.*, 2008), which can regulate Rac/Cdc42 activities via the guanine-nucleotide exchange factor (GEF) PIXα, as reported for mammary epithelial cells (Filipenko *et al.*, 2005). In addition, Rictor could control the activity of Rac/Cdc42 via direct interaction and regulation. Indeed, a study suggested that mTOR binds directly to Rac1 (Saci *et al.*, 2011), but there is no report of Rictor interaction with the Rho GTPase. Alternatively, Rictor might be directly involved in the activation of Rac/Cdc42 GEFs such as DOCK2, PIXα, and P-Rex1. DOCK2 and PIXα regulate Rac/Cdc42 activities in neutrophils (Li *et al.*, 2003; Kunisaki *et al.*, 2006), whereas P-Rex1 coprecipitates with Rictor in HeLa cells and may link mTORC2/Rictor to activation of Rac signaling (Hernandez-Negrete *et al.*, 2007). Finally, Rictor might target negative regulators of Rac/Cdc42 such as GTPase-activating proteins. Of importance, although Rictor depletion profoundly impairs actin polymerization, it is unlikely that Rictor controls Rac activity via actin polymers. This is because an intermediate concentration of latrunculin B exerts a stronger effect on actin polymerization than Rictor depletion but only slightly reduces Rac activity (by ~10%). More complete understanding of the detailed mechanisms by which Rictor and mTOR regulates Rac/Cdc42 activity and the actin cytoskeleton awaits future experiments.

Of note, although the polarization and migratory defects of Rictor depletion in our study are very similar to those reported in an earlier study (Liu *et al.*, 2010), there are discrepancies with respect to the effects of Rictor depletion at the molecular level. For instance, Liu *et al.* (2010) showed that Rictor depletion in dPLB-985 cells reduces F-actin levels at later time points of fMLP stimulation (>1 min), with little effect at the early stage. In contrast, we observed significant decreases in F-actin levels throughout fMLP stimulation. The variation cannot be simply attributed to the differences in cell types, because we used both dHL-60 and dPLB-985 cells and obtained similar results. Furthermore, whereas Liu *et al.* (2010) reported significant increase in RhoA activity upon Rictor depletion with or without fMLP stimulation, the increase in RhoA activity upon Rictor depletion in our experiments is limited to suspended cells with prolonged fMLP stimulation. The following factors might contribute to the discrepancies between the two studies. First, clonal differences between the cell lines may result in the experimental variations. In addition, different shRNAs targeting Rictor were used in these studies and could lead to differential effects in Rictor depletion, as well as in Rictor-mediated signaling pathways. Furthermore, promyeloid leukemia cell lines such as HL-60 and PLB-985 can give rise to variations when induced to differentiate into neutrophil-like cells and/or manipulated genetically, which may lead to the variations between the studies.

It is well established that Rho GTPases can regulate each other's activity through cross-talk during cell polarization and migration (Iden and Collard, 2008). For instance, during migration of slow-moving cells such as fibroblasts, activation of Rac and Cdc42 signaling antagonizes RhoA activity (Sander *et al.*, 1999). Of interest, although depletion of Rictor significantly reduces the level of Rac and Cdc42 in dHL-60 cells, the down-regulation of Rac and Cdc42 activity exerts little effect on RhoA activity, both at early time points after fMLP stimulation in suspended cells and throughout fMLP stimulation in adherent cells. The absence of a clear antagonistic pattern between Rac/Cdc42 and RhoA activities can be attributed to the complex interplay between Rho GTPase in neutrophils during chemotaxis. Van Keymeulen *et al.* (2006) showed that pharmacological inhibition of PI3Kγ in neutrophils not only prevents fMLP-induced Rac and Cdc42 activation, but also significantly reduces RhoA activities. They further proposed that Cdc42 maintains stable polarity by strengthening the leading edge and also, at longer range, by promoting RhoA-dependent actomyosin contraction at the trailing edge (Van Keymeulen *et al.*, 2006). In a separate study, Pestonjamasp *et al.* (2006) used primary human neutrophils and neutrophils derived from a Rac1/Rac2-null transgenic mouse model to show that Rac1 is essential for Rho and myosin activation at the trailing edge to regulate uropod function. Thus Rac and Cdc42 can play both positive and negative roles in the regulation of the RhoA-myosin program during chemotaxis.

Our findings raise the interesting possibility that Rictor might be involved in the compass mechanism that directs actin polymerization at the neutrophil's leading edge. In this highly putative scenario, upon stimulation of chemoattractant, Rictor is recruited to the leading edge, where it activates Rac and Cdc42 and consequently induces localized actin polymerization. The asymmetric accumulation of Rictor in polarized neutrophils and the profound effects of Rictor depletion on neutrophil polarization and motility support this notion. Of note, Rictor depletion in dHL-60 cells leads to profound defects in cell polarization and motility. By contrast, perturbations that lower PI(3,4,5)P3 production only have partial effects on chemotaxis in human and mouse neutrophils. These results suggest that Rictor likely plays a more significant role in regulating leading-edge establishment and polarization of neutrophils than PI(3,4,5)P3. At this point, however, it is unclear whether Rictor is also essential for chemotaxis of neutrophils in response to other chemoattractants, such as C5a and IL-8. It is also unclear whether Rictor plays an instructive or a permissive role in neutrophil polarization. Future experiments should investigate whether localized activation of Rictor is sufficient to induce actin polymerization and neutrophil polarization. An approach that involves the use of rapamycin-binding domain of mTOR (FRB), the protein of interest conjugated with a FK506-binding protein, and the use of small-molecule dimerizers (Inoue *et al.*, 2005; Bayle *et al.*, 2006; Inoue and Meyer, 2008) can be potentially used to induce localized activation of Rictor. This approach was applied to the study of neutrophil polarity and chemotaxis (Inoue and Meyer, 2008).

MATERIALS AND METHODS

Reagents and plasmids

Human fibrinogen, human serum albumin (HSA), and fMLP were from Sigma-Aldrich (St. Louis, MO). Rapamycin, Y-27632, and AKTi-1/2 were from Calbiochem (La Jolla, CA). Torin1 was kindly provided by Nathanael S. Gray (Dana-Farber Cancer Institute, Harvard University, Cambridge, MA) and David M. Sabatini (Whitehead Institute, MIT, Cambridge, MA). Rabbit anti-Rictor antibody, rabbit anti–mSin 1 antibody, and Rictor blocking peptide were from Bethyl Laboratories (Montgomery, TX). Rabbit anti-mTOR antibody, rabbit anti-Raptor antibody, rabbit anti-Akt antibody, mouse anti–phospho [Thr-389]-S6K1, mouse anti–phospho [Ser-473], and rabbit anti–phospho [Thr-308]-Akt antibodies were from Cell Signaling Technology (Beverly, MA). Rabbit anti-RhoGDI2 was from Spring Bioscience (Pleasanton, CA). Alexa Fluor 488–phalloidin, Alexa Fluor 647–phalloidin, and Alexa Fluor 594–conjugated secondary antibodies were from Invitrogen. Goat anti–glyceraldehyde-3-phosphate dehydrogenase (GAPDH) polyclonal antibody and mouse anti–α-tubulin monoclonal antibody were from GenScript (Piscataway, NJ) and Abcam (Cambridge, MA), respectively. All secondary antibodies for Western blotting were from Jackson ImmunoResearch Laboratories (West Grove, PA). Other reagents if not mentioned specifically were from Sigma-Aldrich.

Three shRNA constructs targeting human mTOR (TRCN0000039783, TRCN0000039784, and TRCN0000039785; denoted as mTOR shRNA1, shRNA2, and shRNA3, respectively) and two shRNA constructs targeting human mSin1 (TRCN0000003152 and TRCN0000003153; denoted as mSin1 shRNA1 and shRNA2, respectively) were from Sigma-Aldrich. Two shRNA constructs targeting human Raptor (Id # 1857 and #1858; denoted as Raptor shRNA1 and shRNA2, respectively) or Rictor (Id # 1853 and #1854; denoted as Rictor shRNA1 and shRNA2, respectively) were from Addgene (Cambridge, MA). The shRNA construct targeting the 3′-UTR region of human Rictor (TRCN0000074288) was from Sigma-Aldrich. pCDNA3 vectors containing wild-type mTOR and the kinase-dead mutant are as previously described (Vilella-Bach *et al.*, 1999). The myc-tagged full-length Rictor was from Addgene.

Cell culture, lentiviral infection, and primary neutrophil isolation

Cultivation and differentiation of HL-60 cells and PLB-985 cells were described previously (Wang *et al.*, 2002). Cells were used for experiments on day 6 after dimethyl sulfoxide (DMSO) treatment, when minimal cell death was observed (<1%). For lentiviral production, shRNA-containing plasmids were cotransfected with three packaging plasmids pPL1, pPL2, and pPL/VSVG (Invitrogen, Carlsbad, CA) into HEK293T cells. After 3 d of transfection, supernatant containing the lentiviral particles was concentrated by using Lenti-X concentrator (Clontech, Mountain View, CA), added to HL-60 or PLB-985 cells in the presence of 6 μg/ml Polybrene, and incubated with cells for 18–24 h. Infected cells were transferred to fresh culture medium containing 1.3% DMSO and 0.25 μg/ml puromycin and differentiated for 5 d.

Primary neutrophils were isolated from venous blood from healthy human donors as described (Shin *et al.*, 2010).

Immunofluorescence and live-cell imaging

Procedures for actin staining and immunofluorescence have been described (Shin *et al.*, 2010; He *et al.*, 2011). For live-cell imaging, cells were plated on a human fibrinogen–coated surface for 20 min, washed briefly, and subsequently stimulated with a point source of 10 μM fMLP from a micropipette (Shin *et al.*, 2010; He *et al.*, 2011) or in a microfluidic gradient device with cells attached on the bottom of the entire chamber as described (He *et al.*, 2011).

Apoptosis assay

Apoptosis was measured using the Annexin V FITC Apoptosis Detection Kit (BD Biosciences, Franklin Lakes, NJ) as described (Zhou *et al.*, 2009). Briefly, cells were washed with cold phosphate-buffered saline (PBS) and then resuspended in binding buffer. A 5-μl amount of annexin V–fluorescein isothiocyanate and propidium iodide (PI) was added to and incubated with cells for 20 min at room temperature and subsequently analyzed using a FACSDiva (BD Biosciences). Cells that were annexin V positive and PI negative were counted as apoptotic cells.

Calcium flux

The procedure for measuring the intracellular calcium release after fMLP stimulation was performed as reported previously (Colvin *et al.*, 2006). dHL-60 cells (5×10^6) were suspended in 1 ml of RPMI medium with 1% bovine serum albumin. Cells were incubated with Fura-2 AM (5 μM) at 37°C for 20 min. The cells were washed twice with PBS and suspended in 1 ml of calcium flux buffer (145 mM NaCl, 4 mM KCl, 1 mM $NaHPO_4$, 1.8 mM $CaCl_2$, 25 mM 4-(2-hydroxyethyl)-1-piperazineethanesulfonic acid, 0.8 mM $MgCl_2$, and 22 mM glucose). Fluorescence readings were recorded at 37°C in a fluorimeter (SpectraMax M5; Molecular Devices, Sunnyvale, CA) before and after the addition of fMLP. Intracellular calcium concentrations are presented as the relative ratio of excitation fluorescence intensity emitted at 510 nm in response to sequential excitation at 340 and 380 nm.

Actin polymerization assay

The procedure for measuring polymerized actin was performed as described previously, with some modifications (Weiner *et al.*,

2006). Briefly, 1×10^6 cells were starved in serum-free medium for 1 h at 37°C and suspended in modified Hanks' buffered salt solution (mHBSS) as buffer. Cells were stimulated with 100 nM fMLP for the indicated times. After stimulation, cells were fixed by adding equal volume of 7.4% paraformaldehyde for 30 min at room temperature. Fixed cells were permeabilized and stained in PBS buffer containing 0.1% Triton X-100 and Alexa 488– or 647–conjugated phalloidin (1:100) for 30 min at 37°C in the dark. Stained cells were washed once and suspended in ice-cold PBS, and fluorescence was immediately determined by flow cytometry with a BD Biosciences LSR II System. The mean fluorescence intensity of the cell population was determined. Differentiated PLB cells were stimulated with two concentrations of fMLP (100 nM and 1 µM; the latter concentration was used in previous studies; Liu *et al.*, 2010).

Rac/Cdc42 pull-down assay

Glutathione *S*-transferase–tagged PAK1-PBD (p21-binding domain of PAK1) fusion protein was prepared according to Benard *et al.* (1999). dHL-60 cells (5×10^6) containing NT shRNA or Rictor shRNAs were starved in serum-free medium for 1 h at 37°C. Cells were then suspended in mHBSS buffer and stimulated by 100 nM fMLP for various times. Cell stimulation was stopped by the addition of 1.25× lysis buffer (1× lysis buffer: 25 mM Tris-HCl, pH 7.5, 100 mM NaCl, 5 mM $MgCl_2$, 1% NP-40, 5% glycerol, 1 mM phenylmethylsulfonyl fluoride, 1 mM diisopropyl phosphorofluoridate, and a cocktail of protease inhibitors). Cell lysates were immediately placed on ice. For adhesion condition, cells were plated on fibrinogen (100 µg/ml)-coated six-well plates for 30 min, stimulated with 100 nM fMLP, and then lysed. The subsequent steps were performed as previously described (Benard *et al.*, 1999). Western blotting of Rac, Cdc42, and other proteins was conducted as previously described (Xu *et al.*, 2003; Van Keymeulen *et al.*, 2006; Shin *et al.*, 2010; He *et al.*, 2011). For Rac pull down, the levels of both Rac1- and Rac2-GTP were determined.

RhoA activation assay

An absorbance-based RhoA G-LISA kit (Cytoskeleton, Denver, CO) was used to determine RhoA-GTP levels in dHL-60. Cells with or without Rictor depletion were suspended in mHBSS (5×10^6 cells in 90 µl per condition) and stimulated or unstimulated with 10 µl of 1 µM fMLP. The reaction was stopped by adding 100 µl of 2× lysis buffer (provided with the kit) at 4°C. For adhesion condition, cells were plated on fibrinogen (100 µg/ml)-coated six-well plates for 30 min and then stimulated with 100 nM fMLP for various times. Subsequent steps were performed as described (He *et al.*, 2011).

Statistical analysis

Student's *t* test was used to compare two experimental groups, assuming unequal variances. Differences are considered significant when $p < 0.05$.

ACKNOWLEDGMENTS

We thank Nathanael S. Gray and David M. Sabatini for providing Torin1 and the members of the Wang lab for helpful discussion. This work was supported by National Institutes of Health Grants GM083812 (to F.W.), GM083601 (to C.R. and F.W.), HD059002 (to D.L. and F.W.), and AR048914 and GM089771 (to J.C.), National Science Foundation CAREER Award 0953267 (to F.W.), and the National Science Foundation Science and Technology Center Emergent Behaviors of Integrated Cellular Systems (CBET-0939511).

REFERENCES

Agarwal NK, Chen CH, Cho H, Boulbes DR, Spooner E, Sarbassov DD (2013). Rictor regulates cell migration by suppressing RhoGDI2. Oncogene 32, 2521–2526.

Alessi DR, James SR, Downes CP, Holmes AB, Gaffney PR, Reese CB, Cohen P (1997). Characterization of a 3-phosphoinositide-dependent protein kinase which phosphorylates and activates protein kinase Balpha. Curr Biol 7, 261–269.

Andrew N, Insall RH (2007). Chemotaxis in shallow gradients is mediated independently of PtdIns 3-kinase by biased choices between random protrusions. Nat Cell Biol 9, 193–200.

Barnett SF *et al.* (2005). Identification and characterization of pleckstrin-homology-domain-dependent and isoenzyme-specific Akt inhibitors. Biochem J 385, 399–408.

Bayle JH, Grimley JS, Stankunas K, Gestwicki JE, Wandless TJ, Crabtree GR (2006). Rapamycin analogs with differential binding specificity permit orthogonal control of protein activity. Chem Biol 13, 99–107.

Belham C, Wu S, Avruch J (1999). Intracellular signalling: PDK1—a kinase at the hub of things. Curr Biol 9, R93–R96.

Benard V, Bohl BP, Bokoch GM (1999). Characterization of rac and cdc42 activation in chemoattractant-stimulated human neutrophils using a novel assay for active GTPases. J Biol Chem 274, 13198–13204.

Bhaskar PT, Hay N (2007). The two TORCs and Akt. Dev Cell 12, 487–502.

Bodin S, Welch MD (2005). Plasma membrane organization is essential for balancing competing pseudopod- and uropod-promoting signals during neutrophil polarization and migration. Mol Biol Cell 16, 5773–5783.

Bourne HR, Weiner O (2002). A chemical compass. Nature 419, 21.

Cai H, Das S, Kamimura Y, Long Y, Parent CA, Devreotes PN (2010). Ras-mediated activation of the TORC2-PKB pathway is critical for chemotaxis. J Cell Biol 190, 233–245.

Chen L, Iijima M, Tang M, Landree MA, Huang YE, Xiong Y, Iglesias PA, Devreotes PN (2007). PLA2 and PI3K/PTEN pathways act in parallel to mediate chemotaxis. Dev Cell 12, 603–614.

Colvin RA, Campanella GS, Manice LA, Luster AD (2006). CXCR3 requires tyrosine sulfation for ligand binding and a second extracellular loop arginine residue for ligand-induced chemotaxis. Mol Cell Biol 26, 5838–5849.

Etienne-Manneville S, Hall A (2002). Rho GTPases in cell biology. Nature 420, 629–635.

Ferguson GJ *et al.* (2007). PI(3)Kgamma has an important context-dependent role in neutrophil chemokinesis. Nat Cell Biol 9, 86–91.

Filipenko NR, Attwell S, Roskelley C, Dedhar S (2005). Integrin-linked kinase activity regulates Rac- and Cdc42-mediated actin cytoskeleton reorganization via alpha-PIX. Oncogene 24, 5837–5849.

Franca-Koh J, Kamimura Y, Devreotes PN (2007). Leading-edge research: PtdIns(3,4,5)P3 and directed migration. Nat Cell Biol 9, 15–17.

Frias MA, Thoreen CC, Jaffe JD, Schroder W, Sculley T, Carr SA, Sabatini DM (2006). mSin1 is necessary for Akt/PKB phosphorylation, and its isoforms define three distinct mTORC2s. Curr Biol 16, 1865–1870.

Funamoto S, Milan K, Meili R, Firtel RA (2001). Role of phosphatidylinositol 3′ kinase and a downstream pleckstrin homology domain-containing protein in controlling chemotaxis in *Dictyostelium*. J Cell Biol 153, 795–810.

Gao D *et al.* (2010). Rictor forms a complex with Cullin-1 to promote SGK1 ubiquitination and destruction. Mol Cell 39, 797–808.

Gomez-Mouton C, Lacalle RA, Mira E, Jimenez-Baranda S, Barber DF, Carrera AC, Martinez AC, Manes S (2004). Dynamic redistribution of raft domains as an organizing platform for signaling during cell chemotaxis. J Cell Biol 164, 759–768.

Hauert AB, Martinelli S, Marone C, Niggli V (2002). Differentiated HL-60 cells are a valid model system for the analysis of human neutrophil migration and chemotaxis. Int J Biochem Cell Biol 34, 838–854.

He Y, Kapoor A, Cook S, Liu S, Xiang Y, Rao CV, Kenis PJ, Wang F (2011). The non-receptor tyrosine kinase Lyn controls neutrophil adhesion by recruiting the CrkL-C3G complex and activating Rap1 at the leading edge. J Cell Sci 124, 2153–2164.

Heit B, Liu L, Colarusso P, Puri KD, Kubes P (2008). PI3K accelerates, but is not required for, neutrophil chemotaxis to fMLP. J Cell Sci 121, 205–214.

Hernandez-Negrete I, Carretero-Ortega J, Rosenfeldt H, Hernandez-Garcia R, Calderon-Salinas JV, Reyes-Cruz G, Gutkind JS, Vazquez-Prado J (2007). P-Rex1 links mammalian target of rapamycin signaling to Rac activation and cell migration. J Biol Chem 282, 23708–23715.

Herzmark P, Campbell K, Wang F, Wong K, El-Samad H, Groisman A, Bourne HR (2007). Bound attractant at the leading vs. the trailing edge determines chemotactic prowess. Proc Natl Acad Sci USA 104, 13349–13354.

Hirsch E, Katanaev VL, Garlanda C, Azzolino O, Pirola L, Silengo L, Sozzani S, Mantovani A, Altruda F, Wymann MP (2000). Central role for G protein-coupled phosphoinositide 3-kinase gamma in inflammation. Science 287, 1049–1053.

Hoeller O, Kay RR (2007). Chemotaxis in the absence of PIP3 gradients. Curr Biol 17, 813–817.

Iden S, Collard JG (2008). Crosstalk between small GTPases and polarity proteins in cell polarization. Nat Rev Mol Cell Biol 9, 846–859.

Inoue T, Heo WD, Grimley JS, Wandless TJ, Meyer T (2005). An inducible translocation strategy to rapidly activate and inhibit small GTPase signaling pathways. Nat Methods 2, 415–418.

Inoue T, Meyer T (2008). Synthetic activation of endogenous PI3K and Rac identifies an AND-gate switch for cell polarization and migration. PLoS ONE 3, e3068.

Jacinto E, Facchinetti V, Liu D, Soto N, Wei S, Jung SY, Huang Q, Qin J, Su B (2006). SIN1/MIP1 maintains Rictor-mTOR complex integrity and regulates Akt phosphorylation and substrate specificity. Cell 127, 125–137.

Jacinto E, Loewith R, Schmidt A, Lin S, Ruegg MA, Hall A, Hall MN (2004). Mammalian TOR complex 2 controls the actin cytoskeleton and is rapamycin insensitive. Nat Cell Biol 6, 1122–1128.

Kamada Y, Fujioka Y, Suzuki NN, Inagaki F, Wullschleger S, Loewith R, Hall MN, Ohsumi Y (2005). Tor2 directly phosphorylates the AGC kinase Ypk2 to regulate actin polarization. Mol Cell Biol 25, 7239–7248.

Kamimura Y, Xiong Y, Iglesias PA, Hoeller O, Bolourani P, Devreotes PN (2008). PIP3-independent activation of TorC2 and PKB at the cell's leading edge mediates chemotaxis. Curr Biol 18, 1034–1043.

Knall C, Worthen GS, Johnson GL (1997). Interleukin 8-stimulated phosphatidylinositol-3-kinase activity regulates the migration of human neutrophils independent of extracellular signal-regulated kinase and p38 mitogen-activated protein kinases. Proc Natl Acad Sci USA 94, 3052–3057.

Kunisaki Y *et al*. (2006). DOCK2 is a Rac activator that regulates motility and polarity during neutrophil chemotaxis. J Cell Biol 174, 647–652.

Lee S, Comer FI, Sasaki A, McLeod IX, Duong Y, Okumura K, Yates JR 3rd, Parent CA, Firtel RA (2005). TOR complex 2 integrates cell movement during chemotaxis and signal relay in *Dictyostelium*. Mol Biol Cell 16, 4572–4583.

Li Z *et al*. (2003). Directional sensing requires G beta gamma-mediated PAK1 and PIX alpha-dependent activation of Cdc42. Cell 114, 215–227.

Li Z, Jiang H, Xie W, Zhang Z, Smrcka AV, Wu D (2000). Roles of PLC-beta2 and -beta3 and PI3Kgamma in chemoattractant-mediated signal transduction. Science 287, 1046–1049.

Liu L, Das S, Losert W, Parent CA (2010). mTORC2 regulates neutrophil chemotaxis in a cAMP- and RhoA-dependent fashion. Dev Cell 19, 845–857.

Loewith R, Jacinto E, Wullschleger S, Lorberg A, Crespo JL, Bonenfant D, Oppliger W, Jenoe P, Hall MN (2002). Two TOR complexes, only one of which is rapamycin sensitive, have distinct roles in cell growth control. Mol Cell 10, 457–468.

McDonald PC, Oloumi A, Mills J, Dobreva I, Maidan M, Gray V, Wederell ED, Bally MB, Foster LJ, Dedhar S (2008). Rictor and integrin-linked kinase interact and regulate Akt phosphorylation and cancer cell survival. Cancer Res 68, 1618–1624.

Meili R, Ellsworth C, Lee S, Reddy TB, Ma H, Firtel RA (1999). Chemoattractant-mediated transient activation and membrane localization of Akt/PKB is required for efficient chemotaxis to cAMP in *Dictyostelium*. EMBO J 18, 2092–2105.

Neel NF, Barzik M, Raman D, Sobolik-Delmaire T, Sai J, Ham AJ, Mernaugh RL, Gertler FB, Richmond A (2009). VASP is a CXCR2-interacting protein that regulates CXCR2-mediated polarization and chemotaxis. J Cell Sci 122, 1882–1894.

Nishio M *et al*. (2007). Control of cell polarity and motility by the PtdIns(3,4,5)P3 phosphatase SHIP1. Nat Cell Biol 9, 36–44.

Nuzzi PA, Senetar MA, Huttenlocher A (2007). Asymmetric localization of calpain 2 during neutrophil chemotaxis. Mol Biol Cell 18, 795–805.

Parent CA, Blacklock BJ, Froehlich WM, Murphy DB, Devreotes PN (1998). G protein signaling events are activated at the leading edge of chemotactic cells. Cell 95, 81–91.

Pestonjamasp KN, Forster C, Sun C, Gardiner EM, Bohl B, Weiner O, Bokoch GM, Glogauer M (2006). Rac1 links leading edge and uropod events through Rho and myosin activation during chemotaxis. Blood 108, 2814–2820.

Price LS, Leng J, Schwartz MA, Bokoch GM (1998). Activation of Rac and Cdc42 by integrins mediates cell spreading. Mol Biol Cell 9, 1863–1871.

Rickert P, Weiner OD, Wang F, Bourne HR, Servant G (2000). Leukocytes navigate by compass: roles of PI3Kgamma and its lipid products. Trends Cell Biol 10, 466–473.

Roberts AW *et al*. (1999). Deficiency of the hematopoietic cell-specific Rho family GTPase Rac2 is characterized by abnormalities in neutrophil function and host defense. Immunity 10, 183–196.

Saci A, Cantley LC, Carpenter CL (2011). Rac1 regulates the activity of mTORC1 and mTORC2 and controls cellular size. Mol Cell 42, 50–61.

Sanchez-Madrid F, del Pozo MA (1999). Leukocyte polarization in cell migration and immune interactions. EMBO J 18, 501–511.

Sander EE, ten Klooster JP, van Delft S, van der Kammen RA, Collard JG (1999). Rac downregulates Rho activity: reciprocal balance between both GTPases determines cellular morphology and migratory behavior. J Cell Biol 147, 1009–1022.

Sarbassov DD, Ali SM, Kim DH, Guertin DA, Latek RR, Erdjument-Bromage H, Tempst P, Sabatini DM (2004). Rictor, a novel binding partner of mTOR, defines a rapamycin-insensitive and raptor-independent pathway that regulates the cytoskeleton. Curr Biol 14, 1296–1302.

Sarbassov DD, Ali SM, Sabatini DM (2005a). Growing roles for the mTOR pathway. Curr Opin Cell Biol 17, 596–603.

Sarbassov DD, Guertin DA, Ali SM, Sabatini DM (2005b). Phosphorylation and regulation of Akt/PKB by the rictor-mTOR complex. Science 307, 1098–1101.

Sasaki T *et al*. (2000). Function of PI3Kgamma in thymocyte development, T cell activation, and neutrophil migration. Science 287, 1040–1046.

Schmidt A, Kunz J, Hall MN (1996). TOR2 is required for organization of the actin cytoskeleton in yeast. Proc Natl Acad Sci USA 93, 13780–13785.

Schymeinsky J, Sindrilaru A, Frommhold D, Sperandio M, Gerstl R, Then C, Mocsai A, Scharffetter-Kochanek K, Walzog B (2006). The Vav binding site of the non-receptor tyrosine kinase Syk at Tyr 348 is critical for β2 integrin (CD11/CD18)-mediated neutrophil migration. Blood 108, 3919–3927 .

Servant G, Weiner OD, Herzmark P, Balla T, Sedat JW, Bourne HR (2000). Polarization of chemoattractant receptor signaling during neutrophil chemotaxis. Science 287, 1037–1040.

Shin ME *et al*. (2010). Spatiotemporal organization, regulation, and functions of tractions during neutrophil chemotaxis. Blood 116, 3297–3310.

Srinivasan S, Wang F, Glavas S, Ott A, Hofmann F, Aktories K, Kalman D, Bourne HR (2003). Rac and Cdc42 play distinct roles in regulating PI(3,4,5)P3 and polarity during neutrophil chemotaxis. J Cell Biol 160, 375–385.

Thoreen CC, Kang SA, Chang JW, Liu Q, Zhang J, Gao Y, Reichling LJ, Sim T, Sabatini DM, Gray NS (2009). An ATP-competitive mammalian target of rapamycin inhibitor reveals rapamycin-resistant functions of mTORC1. J Biol Chem 284, 8023–8032.

Van Keymeulen A, Wong K, Knight ZA, Govaerts C, Hahn KM, Shokat KM, Bourne HR (2006). To stabilize neutrophil polarity, PIP3 and Cdc42 augment RhoA activity at the back as well as signals at the front. J Cell Biol 174, 437–445.

Vilella-Bach M, Nuzzi P, Fang Y, Chen J (1999). The FKBP12-rapamycin-binding domain is required for FKBP12-rapamycin-associated protein kinase activity and G1 progression. J Biol Chem 274, 4266–4272.

Wang F (2009). The signaling mechanisms underlying cell polarity and chemotaxis. Cold Spring Harb Perspect Biol 1, a002980.

Wang F, Herzmark P, Weiner OD, Srinivasan S, Servant G, Bourne HR (2002). Lipid products of PI(3)Ks maintain persistent cell polarity and directed motility in neutrophils. Nat Cell Biol 4, 513–518.

Weiner OD (2002). Regulation of cell polarity during eukaryotic chemotaxis: the chemotactic compass. Curr Opin Cell Biol 14, 196–202.

Weiner OD, Rentel MC, Ott A, Brown GE, Jedrychowski M, Yaffe MB, Gygi SP, Cantley LC, Bourne HR, Kirschner MW (2006). Hem-1 complexes are essential for Rac activation, actin polymerization, and myosin regulation during neutrophil chemotaxis. PLoS Biol 4, e38.

Williams DA *et al*. (2000). Dominant negative mutation of the hematopoietic-specific Rho GTPase, Rac2, is associated with a human phagocyte immunodeficiency. Blood 96, 1646–1654.

Wullschleger S, Loewith R, Hall MN (2006). TOR signaling in growth and metabolism. Cell 124, 471–484.

Xu J, Wang F, Van Keymeulen A, Herzmark P, Straight A, Kelly K, Takuwa Y, Sugimoto N, Mitchison T, Bourne HR (2003). Divergent signals and cytoskeletal assemblies regulate self-organizing polarity in neutrophils. Cell 114, 201–214.

Xu J, Wang F, Van Keymeulen A, Rentel M, Bourne HR (2005). Neutrophil microtubules suppress polarity and enhance directional migration. Proc Natl Acad Sci USA 102, 6884–6889.

Yang Q, Inoki K, Ikenoue T, Guan KL (2006). Identification of Sin1 as an essential TORC2 component required for complex formation and kinase activity. Genes Dev 20, 2820–2832.

Zhou J *et al*. (2009). mTOR supports long-term self-renewal and suppresses mesoderm and endoderm activities of human embryonic stem cells. Proc Natl Acad Sci USA 106, 7840–7845.